TWO-PHASE POLYSTYRENE INJECTION WITH SOLIDIFICATION IN RETANGULAR MOLDS USING VOF-TVD METHODOLOGY: INFLUENCES OF TEMPERATURE PROFILE

Carlos E. Fontes
Paulo L. C. Lage
José C. Pinto
Programa de Engenharia Química, COPPE/UFRJ
CP 68502 – CEP 21945-970 – Rio de Janeiro, RJ, Brazil

Abstract. *Simulations of the injection of melt polymer in molds were performed aiming the study of the filling pattern. The fluid flow equations for a pseudo-continuous fluid in a rectangular cavity were solved using Finite-Volume techniques and the SIMPLER scheme. The energy conservation equation was also solved and the interface was tracked by a VOF-TVD scheme. Polymer melt freezing was empirically accounted for in the code. Simulations for melt polystyrene injection in a water filled mold were performed. The influence of the flow initial condition, mold cooling and displaced fluid viscosity on the filing patterns were analyzed. The results show that the displaced fluid viscosity value does not appreciably affect the filling pattern. The initial flow condition slightly affects the filling pattern, while mold cooling can dramatically change the filling pattern.*

Keywords*: Mold filling, TVD schemes, VOF schemes, computational fluid dynamics (CFD), heat transfer.*

1. INTRODUCTION

Injection Molding is an important industrial process for the manufacturing of thin thermoplastic products. During the process, the solid material is heated until it reaches a state of fluidity. It is then injected into the mold cavity under pressure and cooled in the mold. A number of studies have been presented for the simulation of the filling process with varying degrees of complexity, depending upon mathematical formulation of the flow equations, the nature of constitutive equation, the related material properties and the techniques presented to treat the resulting system of equations. Chen and Liu (1989) have done a very good review of the injection molding processes. In this same publication, they have developed a model that treats a two-phase quasi-steady injection. Except for viscosity, all physical fluid properties were considered constant. During the last decade a significant number of researchers have studied problems associated to the filling and post-filling steps of injection molding. Stress patterns (Papathanasiou, 1991), packing and cooling stages (Chen and Liu, 1994), weld-line

formation (Dairanieh et al., 1996 and Chun, 1999), in mold shrinkage (Titomanlio and Jansen, 1996) were some of these issues. However, none of these works has combined transient fluid dynamics analysis with heat transfer and front tracking. All these factors are extremely important in order to have a good simulation of the mold filling phenomena. To the best of our knowledge, the effect of the displaced fluid physical properties on the filling pattern has never been analyzed.

In this work, the conservation equations for mass, momentum and energy have been solved by a finite-volume method using the SIMPLER algorithm, but surface tension effects at the interface were not included in the analysis. The front tracking problem was solved by the VOF (Volume-Of-Fluid) method (Hirt and Nichols, 1981) using a high order TVD-scheme developed by Chakravarthy & Osher (1985) to solve for the color function. The VOF-TVD methodology is described in section 3. A empirical algorithm for melt solidification was also implemented which is able to track the solid-liquid interface during the injection molding simulation.

Melt polystyrene injection was simulated for several conditions which includes different values for the displaced fluid viscosity, different initial flow conditions in a mold and presence or absence of mold cooling. This enables the analysis of the effects of theses variables on the filling pattern.

2. FLUID DYNAMICS EQUATIONS

The used dimensionless 2D-cartesian mass, energy and momentum conservation equation for a pseudo-single-phase Newtonian fluid, with variable density and viscosity, are:

$$\frac{\partial(\varphi)}{\partial\tau} + Re_{ref}\cdot\frac{\partial(\varphi U)}{\partial X} + Re_{ref}\cdot\frac{\partial(\varphi V)}{\partial Y} = 0 \tag{1}$$

$$\frac{\partial(\varphi U)}{\partial\tau} + Re_{ref}\cdot\frac{\partial(\varphi UU)}{\partial X} + Re_{ref}\cdot\frac{\partial(\varphi VU)}{\partial Y} = -Re_{ref}\cdot\frac{\partial P}{\partial X} - \left[\frac{\partial T_{xx}}{\partial X} + \frac{\partial T_{yx}}{\partial Y}\right] \tag{2}$$

$$\frac{\partial(\varphi V)}{\partial\tau} + Re_{ref}\cdot\frac{\partial(\varphi UV)}{\partial X} + Re_{ref}\cdot\frac{\partial(\varphi VV)}{\partial Y} = -Re_{ref}\cdot\frac{\partial P}{\partial Y} - \left[\frac{\partial T_{xy}}{\partial X} + \frac{\partial T_{yy}}{\partial Y}\right] \tag{3}$$

$$\frac{\partial(\varphi\beta\theta)}{\partial\tau} + Re_{ref}\cdot\frac{\partial(\varphi U\beta\theta)}{\partial X} + Re_{ref}\cdot\frac{\partial(\varphi V\beta\theta)}{\partial Y} = \frac{1}{Pr_{ref}}\cdot\left[\frac{\partial}{\partial X}\left(K\cdot\frac{\partial\theta}{\partial X}\right) + \frac{\partial}{\partial Y}\left(K\cdot\frac{\partial\theta}{\partial Y}\right)\right] \tag{4}$$

$$T_{xx} = -2\Gamma\cdot\frac{\partial U}{\partial X} + \frac{2}{3}\cdot\Gamma\cdot\left[\frac{\partial U}{\partial X} + \frac{\partial V}{\partial Y}\right] \tag{5}$$

$$T_{yx} = T_{xy} = -\Gamma\cdot\left[\frac{\partial U}{\partial Y} + \frac{\partial V}{\partial X}\right] \tag{6}$$

$$T_{yy} = -2\cdot\Gamma\cdot\frac{\partial V}{\partial Y} + \frac{2}{3}\cdot\Gamma\cdot\left[\frac{\partial U}{\partial X} + \frac{\partial V}{\partial Y}\right] \tag{7}$$

where

$$X = \frac{x}{Din},\ Y = \frac{y}{Din},\ U = \frac{u}{vmed},\ V = \frac{v}{vmed},\ \tau = \frac{\nu_{ref} \cdot t}{Din^2},\ Re_{ref} = \frac{Din \cdot vmed}{\nu_{ref}} \tag{8}$$

$$P = \frac{p - \rho g_y y - \rho g_x x}{\rho \cdot vmed^2},\ \nu_{ref} = \frac{\mu_{ref}}{\rho_{ref}},\ \Gamma = \frac{\mu}{\mu_{ref}},\ \varphi = \frac{\rho}{\rho_{ref}},\ K = \frac{k}{k_{ref}} \tag{9}$$

$$\beta = \frac{Cp}{Cp_{ref}},\quad \alpha_{ref} = \frac{k_{ref}}{\rho_{ref} \cdot Cp_{ref}},\ Pr_{ref} = \frac{\nu_{ref}}{\alpha_{ref}},\quad \theta = \frac{T}{T_{ref}} \tag{10}$$

and t is the time, x and y are the spatial coordinates, ρ is the density, μ is the viscosity, ν is the kinematic viscosity,α is the thermal diffusivity, k is the thermal conductivity, Cp is the mean specific heat, u is the velocity component in x direction, v is the velocity component in y direction, p is the pressure, T is the temperature, g_i is the body force in i direction, Din is the inlet width and $vmed$ is the mean inlet velocity. The subscript *ref* refers to the inlet fluid properties (fluid 2).

After applying a finite-volume fully implicit discretization on a staggered grid using the power-law scheme, the solution has been achieved using the SIMPLER scheme (Patankar, 1980). The fluidynamics has been tested against benchmark results of channel flow (Gartling, 1990) with good agreement.

3. VOF-TVD SCHEME

Existing methods for the computation of free fluid-fluid interfaces can be classified into two groups (Ferziger & Pèric, 1997): surface fitting and surface capturing methods. For the methods in the first of these categories, the interface is represented and tracked explicitly either by marking it with special marker points, or by attaching it to a mesh surface which is forced to move with the interface. For the methods in the second category, the fluids on both sides of the interface are marked by either massless particles or an indicator (color) function.

The method used in this paper belongs to the second category. In the volume of fluid (VOF) method the advection of the color function F, given by Eq. (11), has to be solved. The F values are stored at in the staggered finite-volume grid similarly to pressure.

$$\frac{\partial F}{\partial \tau} + Re_{ref} \cdot U \cdot \frac{\partial F}{\partial X} + Re_{ref} \cdot V \cdot \frac{\partial F}{\partial Y} = 0 \tag{11}$$

For a given volume, F is equal to 0 when the volume has no injected fluid (in other words, only fluid 1 is inside the mold), but it is equal to 1 when the volume is completely filled with the injected fluid (fluid 2). The interface has F-values between 0 and 1. The dimensionless physical properties of the pseudo-single-phase fluid throughout the mold are given by

$$\varphi = (1-F)\cdot\frac{\rho_1}{\rho_{ref}} + F\frac{\rho_2}{\rho_{ref}},\ \Gamma = (1-F)\cdot\frac{\mu_1}{\mu_{ref}} + F\frac{\mu_2}{\mu_{ref}},\ K = (1-F)\cdot\frac{k_1}{k_{ref}} + F\frac{k_2}{k_{ref}} \tag{12}$$

Numerical diffusion and dispersion are always associated with the solution of Eq. (11). There are some numerical techniques that have been developed to minimize these problems. Among them, there are the modified donor-cell method of Swaminathan and Voller (1994) and the Total Variation Diminishing schemes (TVD). Due to some lack of physical or

mathematical basis in the flux limitation used in the Swaminathan and Voller (1994) scheme, we decided to use a TVD scheme. A good summary of TVD schemes is given by Sweby (1984). A numerical method is TVD if Eq.(13) is valid for scalar conservation laws, where ξ is the transported variable and TV(ξ) is its total variation.

$$TV\left(\xi^{n+1}\right) \le TV\left(\xi^{n}\right), \quad \text{where} \qquad TV(\xi) = \sum_i \left|\xi_i - \xi_{i-1}\right| \tag{13}$$

Chakravarthy & Osher (1985) described one-dimensional second and third-order accurate TVD schemes with low truncation error. These schemes were used to solve advective equations, like Eq. (11), and systems of conservation laws (Euler equations). Goodman and LeVeque (1985) have proved that there is no multidimensional TVD scheme, but Chakravarthy & Osher (1985) have shown that numerical results achieved using their scheme are extremely good. Based on its simplicity and good results the Chakravarthy & Osher (1985) third-order scheme has been used in the present work. All the equations refers to a discretization of Eq. (11) in its non-conservative form. This is due to the characteristics of the chosen TVD scheme which shows large error accumulation if its conservative form is used. Despite all these efforts, numerical diffusion remains relevant most due to low grid density used. Lafaurie et al (1994) propose a renormalization scheme for the color function field in order to decrease the numerical diffusion effect on the front-tracking problem.

The explicit discretized form of Eq.(11) is given by Eq. (14). The *F*-fluxes at the faces of the volumes are determined using the upwind-TVD scheme. For example, for east face, for each *j* line, the flux is given by Eqs. (15) to (22). In these equations the index P means position (i, j), E position $(i+1, j)$, e position $(i+1/2, j)$, ee position $(i+3/2, j)$, w position $(i-1/2, j)$, n position $(i, j+1/2)$, s position $(i, j-1/2)$. When γ equals 1/3 and β equals 4 these equations correspond to a third-order upwind scheme. Equation (15) represents the flux given for the Engquist-Osher first-order scheme for the present flux function (Osher & Chakravarthy, 1984). The minmod function is defined by Eq. (20) and it is used to define the limited fluxes given in Eqs. (18) and (19). The fluxes for the other faces are obtained by obvious changes of subscripts.

$$F_P = F_P^o - \mathrm{Re}_{ref}\,\delta\tau\left[\frac{U_P\cdot\left(F_e^o - F_w^o\right)}{\delta X} + \frac{V_P\cdot\left(F_n^o - F_s^o\right)}{\delta Y}\right] \tag{14}$$

$$U_P F_e = U_i F_{i+\frac{1}{2}} = f_e + h_e \tag{15}$$

$$f_e = f_{i+\frac{1}{2}} = \max[0, U_i]F_i - \max[0, -U_i]F_{i+1} \tag{16}$$

$$h_e = \frac{1}{4}\left[\left(\overline{d\phi}_e^{+} + \overline{\overline{d\phi}}_w^{+}\right) + \gamma\left(\overline{d\phi}_e^{+} - \overline{\overline{d\phi}}_w^{+}\right)\right] - \frac{1}{4}\left[\left(\overline{\overline{d\phi}}_e^{-} + \overline{d\phi}_{ee}^{-}\right) + \gamma\left(\overline{\overline{d\phi}}_e^{-} - \overline{d\phi}_{ee}^{-}\right)\right] \tag{17}$$

$$\overline{d\phi}_e^{+} = \mathrm{minmod}(d\phi_e^{+}, \beta d\phi_w^{+}), \quad \overline{\overline{d\phi}}_w^{+} = \mathrm{minmod}(d\phi_w^{+}, \beta d\phi_e^{+}) \tag{18}$$

$$\overline{\overline{d\phi}}_e^{-} = \mathrm{minmod}(d\phi_e^{-}, \beta d\phi_{ee}^{-}), \quad \overline{d\phi}_{ee}^{-} = \mathrm{minmod}(d\phi_{ee}^{-}, \beta d\phi_e^{-}) \tag{19}$$

$$\text{minmod}(a,b) = \text{sign}(a) \cdot \max\left\{0, \min\left[|a|, b\,\text{sign}(a)\right]\right\} \tag{20}$$

$$d\phi_e^+ = d\phi_{i+\frac{1}{2}}^+ = U_i \cdot (F_{i+1} - F_i), \qquad U_i > 0 \tag{21}$$

$$d\phi_e^- = d\phi_{i+\frac{1}{2}}^- = U_i \cdot (F_{i+1} - F_i), \qquad U_i \le 0 \tag{22}$$

Boundary conditions for this equation are obvious: the cells at the inlet outside the mold are considered to be completely filled with fluid 2 (F = 1), all cells after the outlet are considered to be completely filled with fluid 1 (F = 0) and there is no F flux at the other boundaries. In the beginning of the filling process, the mold is filled with fluid 1 (F = 0).

4. SOLIDIFICATION CONDITIONS

During the filling, the melt cooling produces a huge viscosity increase what causes the reduction of velocity and, finally, solidification. In order to numerically simulate the solidification process, the following heuristic has chosen: the fluid in a cell is considered to become a solid if all velocity components at its four faces become smaller than 0.05m/s, the fluid viscosity become higher than 1000 Pa.s and the cell makes a boundary with the wall or another solidified cell. After solidification of a computational cell, only the energy equation is solved for it. The algorithm also allows fluid melting in a previously solidified cell if its temperature changes accordingly. Since the solid polymer is a subcooled liquid, there is no sharp phase change, being not necessary to consider the heat of solidification in the analysis.

5. BOUNDARY AND INITIAL CONDITIONS

Fully-developed laminar velocity profile was assumed for v at the inlet boundary, as given by Eq. (30):

$$v(x) = A \cdot (B - x)(x - C) \qquad \text{for } B \le x \le C \tag{30}$$

At the outlet boundary, the pressure and the horizontal component of velocity were set to zero and continuity conditions were adopted for vertical velocity component at this position. The non-slip condition has been used on all solid walls. Constant A in Eq. (30) was calculated in order to guarantee an average inlet velocity equal to 0.1 m/s.

Large differences in the physical properties of the polymer and the displaced fluid bring about numerical difficulties. In order to analyze the effects of these property variations, two systems were analyzed: water-polystyrene and fluid A-polystyrene. Fluid A is a fictitious fluid which has all properties equal to those of air but the density used in the fluid dynamic equations which was made equal to the water density.

Another point that has to be addressed was the initial flow condition of the fluid inside the mold. Depending on the actual injection equipment and mold, it can range from the no flow condition, when the polymer is immediately injected in the mold, to the steady-state conditions, when there is a considerable amount of fluid 1 (usually air) in the tubes of the injection equipment which is forced to flow throughout the mold.

The actual initial flow condition is something in between these two limits, that is, it is a developing flow which may only be calculated if the whole equipment is modeled. Thus, some simulations have been performed with water-polystyrene system to compare the results with these two limits for the flow initial condition.

Table 1- Physical properties of the fluids.

Fluid	ρ (kg/m^3)	ρ*Cp* (kJ/m^{3}K)	*k* (10^{-3} W/m.K)	μ (Pa.s)
polystyrene	$1250 - 0.65 \cdot T$	1.88 ρ	126	$\exp(-13.23 + 6557T^{-1})$
Water	990	4140	645	5.3×10^{-4}
Fluid A	990	1.17	28	1.9×10^{-5}

In all simulations, is was assumed that the mold walls were kept at a given temperature (283 K) while the injected fluid is at 373 K. A possible initial temperature condition for the fluid inside the mold would be the wall temperature, as if it were in thermal equilibrium with the mold before the injection begins. However, this condition leads to a temperature discontinuity what brings an extra physical property jump. The algorithm could not manage well this situation and the solution was to set the initial internal temperature equal to the inlet fluid temperature (373 K).

6. SIMULATION RESULTS

All the simulations presented in the following have been obtained for the filling of a square mold with one inlet and one outlet, as shown in Figure 1 (LX = LY). In this figure, Din and Dout are, respectively, the inlet and outlet lengths. They both equals 20 mm. Dimensions LX and LY equals 0.1 m. The physical properties of the fluids are summarized in Table 1. Polystyrene properties were achieved from Fontes et al (1997). All the other properties were obtained from Incropera & De Witt (1990). All the water physical properties were evaluated at a mean temperature of 325K and considered constant. Only polystyrene density and viscosity were considered temperature dependent. Fluid A properties corresponds to air properties at 325 K and 1 atm except the density used in the fluid dynamics equations, where a value equal to the water density was used.

The SIMPLER algorithm has been developed for moderate changes of the fluid density. Since the values for water and polystyrene densities are similar, this algorithm is capable of solving our system of equations. However, the energy balance used the real value of ρCp product, as given by Table 1, what means that the real value for the polystyrene density is always used in the energy equation.

Table 2 lists the conditions used in the simulations. Case 1 refers to simulations without heat transfer, when the whole system is adiabatic and kept at the inlet temperature of 373 K. In this case, all properties were considered constant and evaluated at mean temperature of 325K. Cases 2 and 3 correspond to polystyrene injection at inlet temperature of 373 K. The fluid inside the mold is assumed to have an initial temperature equal to the inlet temperature and the mold walls are kept at 283 K. For these simulations, polystyrene properties are evaluated as given in Table 1. Cases 1 and 2 assume that, initially, the fluid inside the mold is flowing at steady-state conditions. Case 3 assumes an initial stagnant fluid inside the mold.

For all simulations, a 15×15 grid has been used. Although quite coarse, we believe that this mesh captures the mold filling pattern. For the water-polystyrene injection simulations, due to the large differences in viscosity between the two fluids, it was necessary to use quite small time steps (10^{-5} to 10^{-6}) to guarantee the mass balance closure. Although the 3rd-order TVD scheme has low numerical diffusion, it is present in the following results due to the coarse mesh used.

All the results that are presented below for the mold filling patterns are shown in a contour-level plot where only the F = 0.5 level was plotted. The black region is filled with

polystyrene and the white region represents the other fluid. Unless otherwise stated, these and the following figures show water-polystyrene simulations results at t = 5s.

Table 2 – Simulation conditions.

Case	Mold Cooling	Initial Condition
1	No	Steady-State
2	Yes	Steady-State
3	Yes	Stagnant Fluid

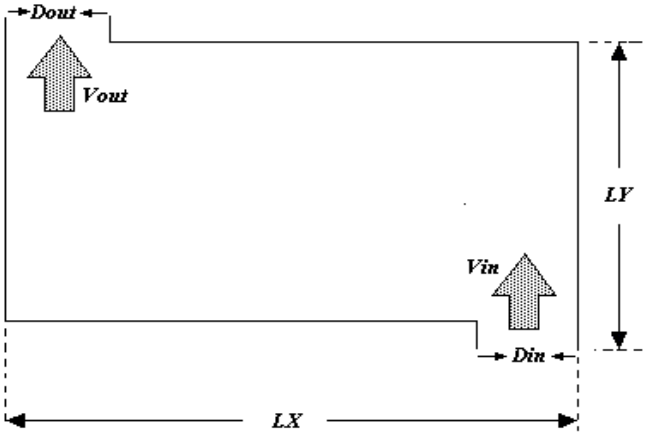

Figure 1- Two-dimensional rectangular mold.

Figure 2 compares filling patterns and streamlines for Case 1 simulations for the water-polystyrene system. In Figure 2-a the correct value for water viscosity was used, but in Figure 2-b its value was two orders of magnitude smaller (even smaller than the air viscosity value). The same filling patterns are achieved. This justify the usage of a constant value for the viscosity for fluid 1.

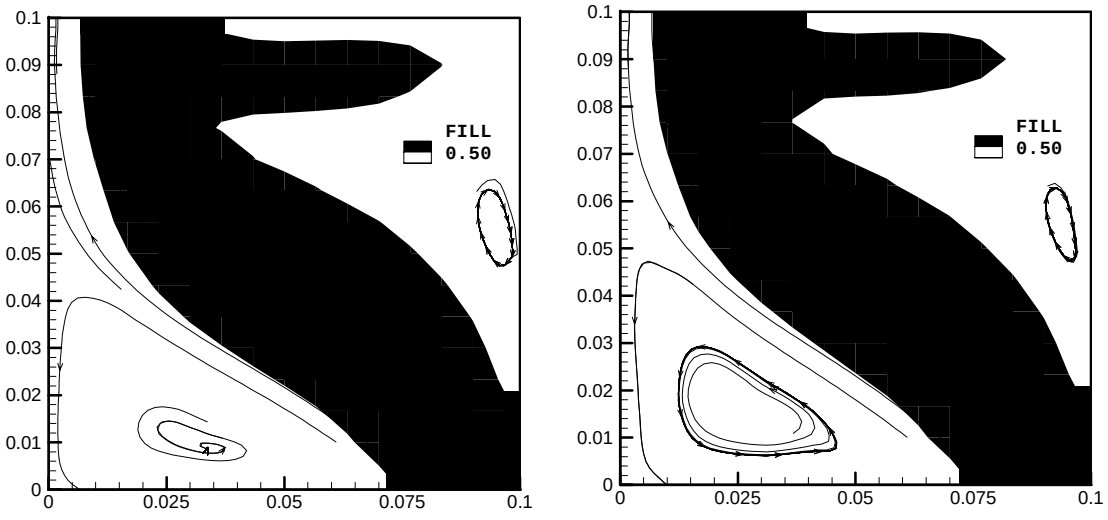

(a) (b)

Figure 2 – Filling patterns and streamlines for water-polystyrene injection: case 1.
(a) Water (b) Fluid A

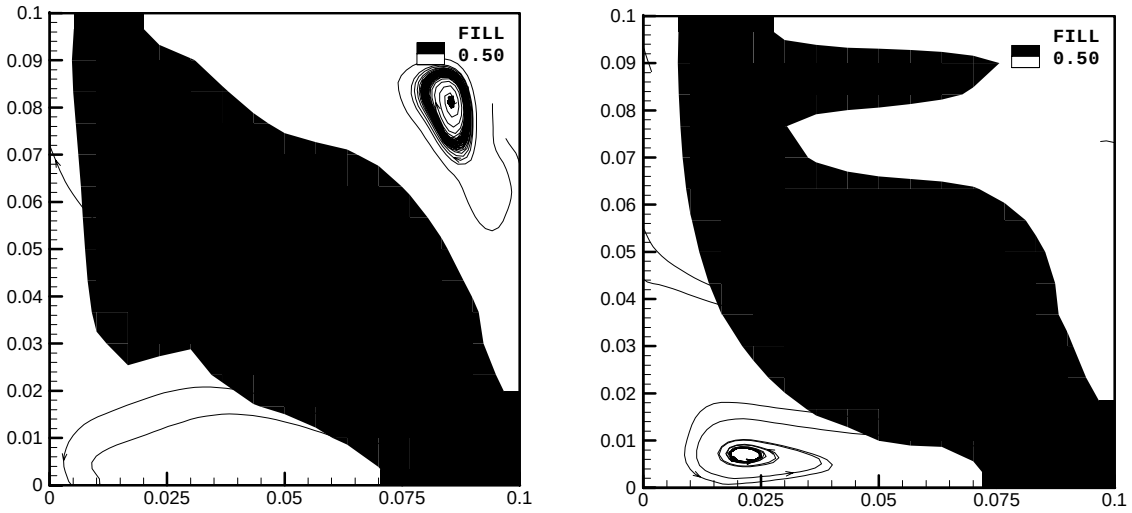

(a) (b)

Figure 3 - Filling patterns and streamlines for water-polystyrene injection: (a) case 2 and (b) case 3.

Figure 3 compares water-polystyrene simulations for Cases 2 and 3 of Table 2, showing that there exists some difference in the filling patterns for the two limiting cases for the initial flow condition inside the mold. However, the difference in the filling patterns is small. Since the use of a steady-state initial condition leads to a much smaller computation effort, it seems useful to use it for mold-filling simulations.

Figure 4 compares water-polystyrene simulations for Cases 1 and 2 of Table 2. It clearly shows that, for this 2-D simulation, mold cooling modifies appreciably the filling pattern, which happens due to the dependence of polymer viscosity on temperature. Figure 5 shows the temperature profile for the moment described at Figure 4-b.

Our results have shown that there is no significant solidification during the filling unless you use very low wall temperatures. In order to evaluate this situation and the code capability to predict it, a simulation was performed for fluid A-polystyrene injection (see Table 1). The magnitude of the ρCp product for fluid A is the same for air, what means that there is much less thermal inertia and the internal mold temperature decreases faster in this system, leading

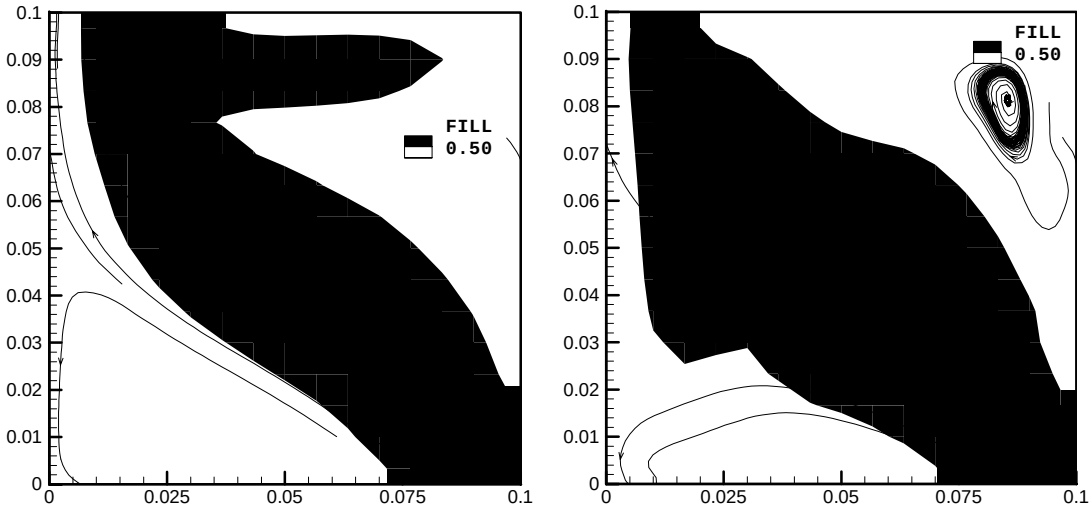

(a) (b)

Figure 4 - Filling patterns and streamlines for water-polystyrene injection: (a) case 1 and (b) case 2.

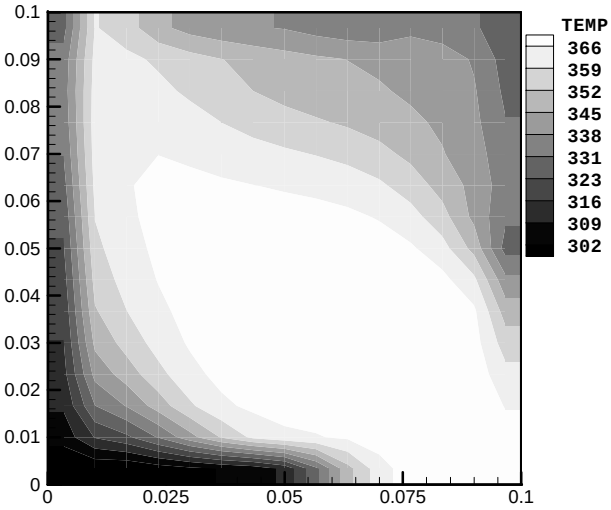

Figure 5 - Temperature profile for Figure 4-b

to polymer freezing. Figure 6 shows that the inlet flow of the mold may be disturbed by polymer solidification near the injection point for fluid A-polystyrene mold filling for Case 2 conditions. The wall temperature was 250 K. This figure was produced at t = 2 s.

The above results show that the heat transfer effect during the mold filling may be very important even in these 2-D simulations. The reduction of flow cross section area due to polymer solidification close to the wall, could be verified in these 2-D simulations (Figure 6). However, its effect on fluid flow was small. Actual molds need 3-D simulations, where the fountain flow is a phenomena that cannot be forgotten.

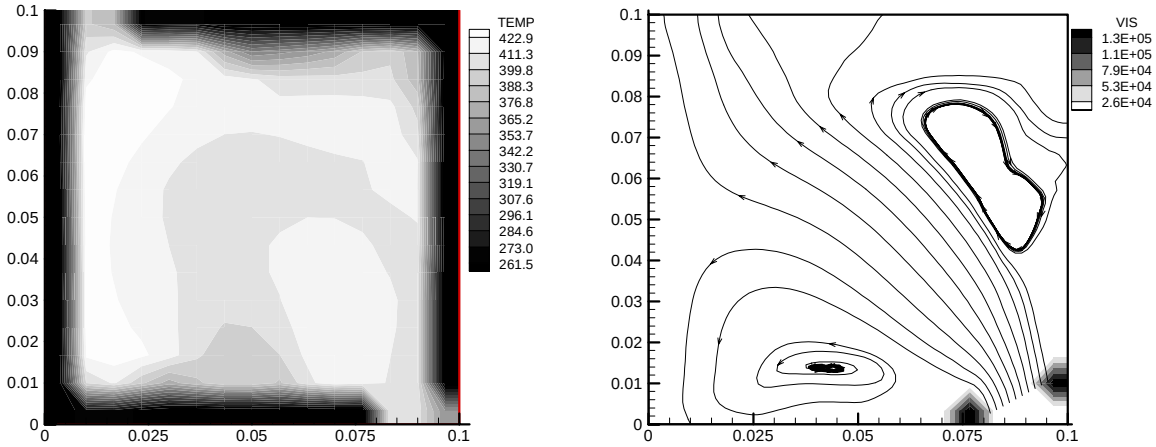

(a) (b)

Figure 6 - Fluid A-polystyrene injection: (a) temperature profile, (b) viscosity profile.

6. CONCLUSIONS

Simulations of polystyrene injection in a 2-D mold were performed. The displaced fluid was water or a fictitious fluid with all properties, but the density, similar to those of air. The effects of initial flow condition, the displaced fluid viscosity and mold cooling in the filling patterns were analyzed. Our results have shown that the value used for the displaced fluid viscosity does not affect appreciable the filling pattern. Steady-state initial flow condition or stagnant fluid initial condition lead to filling patterns slightly different. This implies that the flow in the whole equipment should be modeled for a more accurate description of the mold

filling. Injection with mold cooling leads to quite different filling patterns due to viscosity changes. Moreover, when the polymer freezes, flow cross-section area contraction can modify appreciably the filling patterns.

ACKNOWLEDGEMENTS

The authors acknowledge the financial support obtained from CAPES and from CNPq, grant number 520660/98-6.

REFERENCES

Chakravarthy, S.R. & Osher,S., 1985, A New Class of High Accuracy TVD Schemes for Hyperbolic Conservation Laws, AIAA paper 85-0363

Chen, B.S. & Liu, W.H., 1989, Numerical Simulation and Experimental Investigation of Injection Molding Filling With Melt Solidification, Polymer Eng. and Science, vol.29, nº15, p. 1039-1050.

Chen, B.S. & Liu, W.H., 1994, Numerical Simulation of the Post-Filling Stage in Injection Molding Filling With a Two-Phase Model, Polymer Eng. and Science, vol.34, nº10, p. 835-846.

Chun, D.H., 1999, Cavity Filling Analysis of Injection Molding Simulation: Bubble and Weld Line Formation, Computational Materials Science 16: (1-4) 151-157.

Dairanieh, I.S., Haufe, A., Wolf, H.J. and Menning, G., 1996, Computer Simulation of Weld-Lines in Injection Molded Poly(Methyl Methacrylate), Polymer Eng. and Science, vol.36, nº15, p. 2050-2057.

Ferziger, J.H & Peric, M., 1997, Computational Methods for Fluid Dynamics, Springer, New York

Fontes, C.E., Lage, P.L.C., & Pinto, J.C., 1997, Modelagem e Simulação da Homopolimerização de Estireno em Massa em Moldes Cilíndricos PEQ/COPPE/UFRJ.

Gartling, D.K., 1990, A Test Problem for Outflow Boundary Conditions - Flow over a Backward Facing Step, International Journal for Numerical Methods in Fluids, vol.11, pp 953-967.

Goodman, J.B. & LeVeque, R.J., 1985, On the Accuracy of Stable Schemes for 2-D scalar Conservation Laws, Math. Comp., vol. 45, p.15

Hirt,C.W. & Nichols, B.D., 1981, Volume of Fluid (VOF) Method for the Dynamics of Free Boundaries, Journal of Computational Physics, vol.39, pp.201-225

Incropera & De Witt, 1990, Fundamentals of Heat Transfer, 3rd ed., John Wiley & Sons.

Lafaurie, B., Nardone, C., Scardovelli, R., Zaleski, S. and Zanetti, G., 1994, Modelling Merging and Fragmentation in Multiphase Flows with SURFER, J. of Comp. Physics 113, 134-147

Osher, S., & Chakravarthy, S., 1984, Very High Order Accurate TVD Schemes, ICASE Report no. 84-44, ICASE – NASA Langley Research Center, Hampton, Virginia.

Papathanasiou, T.D., 1991, D.Sc. Thesis, Dep. of Chemical Engineering, MacGill University, Montreal, Quebec, Canada.

Patankar, S.V., 1980, Numerical Heat Transfer and Fluid Flow, McGraw-Hill, New York.

Swaminathan,C.R. & Voller, V.R., 1994, A Time-Implicit Filling Algorithm, Appl. Math. Modelling, vol.18, pp 101-108

Sweby, P.K., 1984, High Resolution Schemes Using flux Limiters for Hyperbolic Conservation Laws, SIAM Journal of Numerical Analysis, vol.21, n.5, pp. 995-1011

Titomanlio, G. & Jansen, K.M.B., 1996, In-mold Shrinkage and Stress Prediction in Injection Molding, Polymer Eng. and Science, vol.36, nº15, p. 2041-2049.